

AD _____

USAARL REPORT NO. 77-5

THE IN VIVO DYNAMIC MATERIAL PROPERTIES OF THE CANINE SPINAL CORD

By

Y. King Liu, Ph.D.
K. B. Chandran, D.Sc.
J. K. Wickstrom, M.D.

Tulane University School of Medicine
New Orleans, LA 70112

December 1976

Final Report

Distribution Statement: This document has been approved for public release and sale; its distribution is unlimited.

U. S. ARMY AEROMEDICAL RESEARCH LABORATORY

Fort Rucker, Alabama 36362



DD FORM 1473 EDITION OF 1 NOV 65 IS OBSOLETE

a probe attached to an electromagnetic vibrator. At two other locations, signals were monitored by pressure transducers pressed gently against the cord. The speed of the wave propagation was determined at various frequencies from the measured time lag and the distance between the transducers. Assuming a model of an elastic tube filled with inviscid fluid, the Young's modulus for the dura in the circumferential direction was computed via the so-called Moens-Korteweg equation. Similar measurements were made on the axial and torsional waves. These waves were induced by attaching a specially designed adapter to the vibrator. The propagation of these waves was monitored at two other locations, where targets with an optical discontinuity (black and yellow interface) were mounted. The movement of these targets as a result of the wave transit, were followed by an electro-optical tracking system. The results showed that the spinal dura mater behaved like an anisotropic medium, being stiffest when loaded normal to its surface and softest under torsional loading. Based on the experimental data, mean values for the circumferential and axial Young's moduli and shear modulus, useful for the frequency range of these tests were recommended.

NOTICE

Qualified requesters may obtain copies from the Defense Documentation Center (DDC), Cameron Station, Alexandria, Virginia. Orders will be expedited if placed through the librarian or other person designated to request documents from DDC (Formerly ASTIA).

Change of Address

Organization receiving reports from the US Army Aeromedical Research Laboratory on automatic mailing lists should confirm correct address when corresponding about laboratory reports.

Disposition

Destroy this report when it is no longer needed. Do not return it to the originator.

Distribution Statement

This document has been approved for public release and sale; its distribution is unlimited.

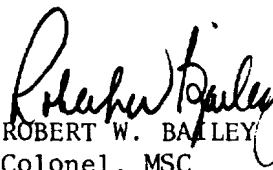
Disclaimer

The findings in this report are not to be construed as an official Department of the Army position unless so designated by other authorized documents.

SUMMARY

A wave propagation study was completed to determine the in vivo dynamic material properties of the dura mater in mongrel dogs. A portion of the thoracic spinal cord was exposed by laminectomy. The dog was artificially respired after its muscles were paralyzed to prevent any jerk reflex initiated by the spinal cord during the experiment. In the pressure wave experiments, sinusoidal pressure signals were induced on the in vivo and in situ spinal cord with a probe attached to an electromagnetic vibrator. At two other locations, signals were monitored by pressure transducers pressed gently against the cord. The speed of the wave propagation was determined at various frequencies from the measured time lag and the distance between the transducers. Assuming a model of an elastic tube filled with inviscid fluid, the Young's modulus for the dura in the circumferential direction was computed via the so-called Moens-Korteweg equation. Similar measurements were made on the axial and torsional waves. These waves were induced by attaching a specially designed adapter to the vibrator. The propagation of these waves was monitored at two other locations, where targets with an optical discontinuity (black and yellow interface) were mounted. The movement of these targets as a result of the wave transit, were followed by an electro-optical tracking system. The results showed that the spinal dura mater behaved like an anisotropic medium, being stiffest when loaded normal to its surface and softest under torsional loading. Based on the experimental data, mean values for the circumferential and axial Young's moduli and shear modulus, useful for the frequency range of these tests were recommended.

Approved:


ROBERT W. BAILEY
Colonel, MSC
Commanding

FOREWORD

This report was submitted to the U.S. Army Aeromedical Research Laboratory in fulfillment of Contract No. DABT01-75-C-0237

TABLE OF CONTENTS

	PAGE
ABSTRACT	
LIST OF FIGURES	
INTRODUCTION	1
BRIEF REVIEW OF PREVIOUS WORK	1
THEORETICAL BACKGROUND OF THE PRESENT PROPOSAL	2
EXPERIMENTAL METHODS AND APPARATI	4
Animal Preparation	4
Experimental Procedure	4
Data Reduction and Error Analysis	11
Computation of Elastic Moduli	17
Results and Discussion	17
SUMMARY AND RECOMMENDATION	29
REFERENCES	30
APPENDIX A	32

LIST OF FIGURES

FIGURE NO.

1. Dog after laminectomy showing the exposed spinal cord.
2. Schematic of the experimental set up to induce and monitor waves on the spinal cord.
3. Set up of the vibrator and pressure transducers mounted on a stand to measure the pressure wave propagation.
4. Recordings of pressure waves (top signal is the input, the middle signal is picked up by the proximal transducer and the bottom signal is picked up by the distal transducer. The sensitivities and the time scale setting of the scope are indicated on the side of the Figure).
5. Adapter attached to the electromagnetic vibrator to induce torsional and axial waves.
6. Optron electro-optical tracker system for monitoring the torsional waves.
7. Recording of axial waves (top signal is the input, the middle signal is picked up by the proximal target and the bottom signal is picked up by the distal target. The sensitivities and the time scale setting of the scope are indicated on the side of the Figure).
8. Recordings of torsional waves (top signal is the input, the middle signal is picked up by the proximal target and the bottom signal is picked up by the distal target. The sensitivities and the time scale setting of the scope are indicated on the side of the Figure).
9. Schematic of the time lag measurement.
10. Wave speed as a function of frequency for pressure waves.
11. Young's modulus, E_p , as a function of frequency for pressure waves.
12. Wave speed as a function of frequency for torsional waves.
13. Shear modulus, G , as a function of frequency for torsional waves.
14. Wave speed as a function of frequency for axial waves.
15. Young's modulus, E_a , as a function of frequency for axial waves.

FIGURE NO.

- A1 Analysis of Photograph
- A2 Digitizer Program Flow Chart
- A3 Digitizer Program Listing

INTRODUCTION

Spinal cord injuries, particularly those which result in paraplegia and quadriplegia, present an economic problem of staggering magnitude. The chief cause of these injuries are automobile, industrial and sports accidents. In addition, war casualties are also a major contributor for these traumatic injuries.

The greatest deficit in experimental studies is the lack of investigations linking the mechanics of the input trauma to the sequence of physiopathologic responses. A fairly large effort on the material properties of the in vitro vertebrae and discs has been supported by such federal agencies as the Departments of Defense and Transportation, as well as the National Institutes of Health. However, knowledge of the dynamic, in vivo, in situ material properties of the spinal cord itself is practically nonexistent. Without this class of data, our pathophysiologic understanding would at best be qualitative and thus incomplete. The purpose of the present study is to fill in this gap in our quantitative knowledge and understanding of the response of the spinal cord under dynamic loads.

This report describes in detail the determination of the in vivo dynamic material properties of the canine spinal cord from its wave transmission characteristics. Sinusoidal pressure, axial and torsional waves were induced on the exposed spinal cord of a dog and the waves monitored at two other locations at a fixed distance from each other. The pressure, axial and torsional wave speeds computed from the above measurements are used to yield values for the elastic moduli of the dura mater. Since the central nervous system (CNS), consisting of the cortex, brainstem, spinal cord and cauda equina, is a closed, integral functional unit, the material properties determined from the dura invested brain tissue at the spinal cord level should also shed much light on the material behavior for the rest of the system.

BRIEF REVIEW OF PREVIOUS WORK

Extensive investigations have been reported on wave propagation characteristics on fluid filled elastic/viscoelastic tubes mainly as a model for blood flow in the circulatory system. Some typical publications are those of Womersley (1957), Atabek (1968) and Maxwell and Anliker (1968). The theory of wave propagation has also been successfully applied in in vivo experimental analysis of the behavior of the blood vessels in dogs and a detailed review is found in Anliker (1972).

The dura mater has been tested in vitro. McElhaney et al. (1973) reported a mean Young's modulus of approximately 6000 psi under quasi-static conditions and 8800 psi at a strain rate of 6.66 sec^{-1} . The viscoelastic description of the brain material, which is also contained in the spinal cord, has been achieved through in vitro testing. The two quantities of interest are the complex bulk modulus and the complex shear modulus. There is general consensus, see McElhaney et al. (1973),

that the bulk modulus is about 300,000 psi and independent of frequency; i.e., the brain has an elastic response to hydrostatic loading. Fallenstein et al. (1969) subjected rectangular specimens of brain to a sinusoidally varying shear stress and measured the resulting strain. They obtained a real part in the range of 0.09 to 0.16 psi and a loss tangent (the ratio of the imaginary to the real part) from 0.40 to 0.55 in the frequency range of 9-10 Hz. Shuck and Advani (1972) imposed a uniform steady state angular displacement on one base of a brain-filled cylinder and measured the torque magnitude and phase transmitted through the cylinder. The theoretical analysis of the experiment allowed the computation of the imaginary and real parts of the complex shear modulus to be calculated. The test was conducted at a frequency range of 1-350 Hz. The values reported by Shuck and Advani (1972) differed from Fallenstein et al. (1969) by an order of magnitude. It is fairly easy to show that for an impact of several milliseconds duration, it is necessary to know the shear modulus function over the frequency range of 0-2200 Hz.

While the in vitro work cited above is important and necessary, one cannot infer that their combination must ipso facto be their in vivo behavior. Three factors can contribute to the discrepancy: (i) The spinal cord is axially tethered, see Breig (1960); (ii) The spinal cord matter and the dura mater are both viscoelastic; and (iii) The soft tissue pressure on the spinal cord from its surroundings. Thus, the need for in vivo experiments is clearly obvious.

THEORETICAL BACKGROUND OF THE PRESENT PROPOSAL

With the values obtained from the in vitro experiments mentioned above, the spinal cord can be idealized as a thin-walled viscoelastic membrane tapered tube filled with an inviscid and incompressible fluid. The wall of the dura mater is assumed to have isotropic, homogeneous and viscoelastic properties. Classical wave propagation theory and experiments have been applied to determine its material properties, as has been shown by Anliker (1972). Three types of waves are present when such a system is disturbed:

$$(a) \quad c_p = (Eh/2\rho_f a)^{\frac{1}{2}}, \quad (1)$$

where E is the Young's modulus in the circumferential direction of the vessel wall, h is the wall thickness of the vessel, ρ_f is the density of the fluid and a is the radius of the tube.

$$(b) \quad c_a = [E/\rho_s (1-\nu^2)]^{\frac{1}{2}}, \quad (2)$$

where ρ_s is the density of the wall and ν , its Poisson's ratio.

$$(c) \quad c_t = (G/\rho_s)^{\frac{1}{2}} \quad (3)$$

where G is the shear modulus of the wall. These waves are referred to

as the pressure, axial and torsional waves according to their predominant physical characteristics. The pressure waves are characterized by a strong interaction between the "fluid" and the tube wall, whereas the axial and torsional waves exhibit very little fluid-membrane interaction. It is possible to induce small transient signals in which one of the three waves are dominant and measure its phase velocity, dispersion and attenuation properties as a function of the applied frequencies. By selecting transient signals in the form of a finite train of sine waves, the need for Fourier transform computation is eliminated if the wall medium is mildly dispersive, i.e., the phase velocity is changed by a few percent when the frequency is changed by 10%. Since the Fourier spectrum of the input signal is dominated in proportion to the length of the train at the input frequency, the speed of the transient signal is a good approximation to the phase velocity at the given frequency.

The wave transmission characteristics described above have been extensively studied on fluid-filled latex rubber tubes by Klip et al. (1967). However, careful consideration must be given in applying the theory to physiological conditions in vivo. In physiological systems like the spinal cord, we would expect a wave velocity of the order of 5 to 10 m/sec. From the relation

$$c = n\lambda, \quad (4)$$

where c is the wave speed, n is the frequency and λ is the wave length, we know that at a frequency of 1 Hz, the wave will travel a distance of 5 to 10 m in one second. In an experiment when approximately 10 cm of spinal cord is exposed, one will encounter multiple reflections and distortions of the wave shape at low-frequency input pulses. These reflections make the determination of the phase velocities and attenuation a much more complicated task. Moreover, Maxwell and Anliker (1968), have shown that in blood vessels, pressure waves of high frequencies and small amplitudes are dissipated primarily by the viscoelastic behavior of the wall. In light of the above considerations, it is thus, preferable to perform the wave propagation studies in vivo at high frequencies in the order of 100 Hz, than at the lower frequencies. At 100 Hz, the input sine wave would theoretically have little or no distortion if the pressure transducers are placed 5 to 10 cm apart. The assumption that the spinal cord is a viscoelastic tapered tube consisting of inviscid incompressible fluid is also justified if limited to high frequencies. Additionally, the material properties for the high strain rates encountered in trauma, correspond to precisely its high frequency response. Guided by the above considerations, we performed a feasibility study (Final Report of Contract DAMD17-74-G-9384) to establish the animal surgical procedure and also to determine the required electromechanical equipment for the project. This report by Liu et al. (1975) was part of the previous contract, of which the present contract is a logical continuation.

EXPERIMENTAL METHODS AND APPARATI

1. Animal Preparation

Medium-sized mongrel dogs used in this study were suitably anesthetized by sodium pentobarbital injected i. v. at the following dosage: 1 cc (50 mg/cc) per 5 lb. weight of the dog. Cannulation of the femoral vein was performed so that future injections of anesthetic, other drugs or saline can be quickly accomplished, if and when necessary, during the course of the experiment. The dog was also connected to a respirator either through a tracheostomy or by tracheal intubation. Surgery consisted of exposing a portion of the spinal cord in the thoracic region of the dog through a posterior approach. The process was very similar to a laminectomy, a standard surgical procedure. Fig. 1 shows the exposed portion of a canine spinal cord after the surgery was completed. During the surgery, excessive bleeding was kept to a minimum through the use of a Valley Lab. Model SSC 1 coagulator. Replacement saline, at body temperature, is periodically injected through the venous cannula to maintain homeostasis. Just before the actual experiment with the spinal cord, Decamethonium[®] at a dosage of 1 cc (0.01 mg/cc) per 10 lbs weight of the dog was injected to paralyze the muscles. The animal was connected to a respirator upon fasciculation of the respiratory muscles.

2. Experimental Procedure

(a) Pressure Waves:

Sinusoidal pressure waves were induced by pressing a metal probe of 1/4" diameter connected to a vibrator (Ling Electronics, Model 203). The vibrator was in turn connected to a sine wave generator (Heathkit IG-18) through a tone burst generator (General Radio 1396-B). The tone burst generator was included in the set up so that a finite train of sine waves can be delivered to activate the vibrator for each measurement. The reason for using finite train waves was discussed in detail by Moritz (1969) and is omitted here in the interest of brevity. We generally have used a train of 4 sine waves in our experiments.

A schematic of the experimental set up is shown in Fig. 2. Through this arrangement sinusoidal signals of variable amplitudes and frequencies can be applied, for a given time duration, to the probe. The pressure waves thus induced on the spinal cord were monitored through Entran micro pressure transducers (Model EPA 125E-5) mounted on 1/4" diameter aluminum probes at the factory. These transducers were connected to an Astrodata signal conditioner-amplifier system, which in turn was connected to a four channel storage oscilloscope (Tektronix Model 5103N). The input signal was displayed along with the two pressure signals picked up. The transducers were mounted on a specially constructed stand, which can be adjusted such that the transducers are positioned with a slight pressure on the cord. The distance between the two transducers are measured on a scale mounted on the stand. A picture of the setup is shown

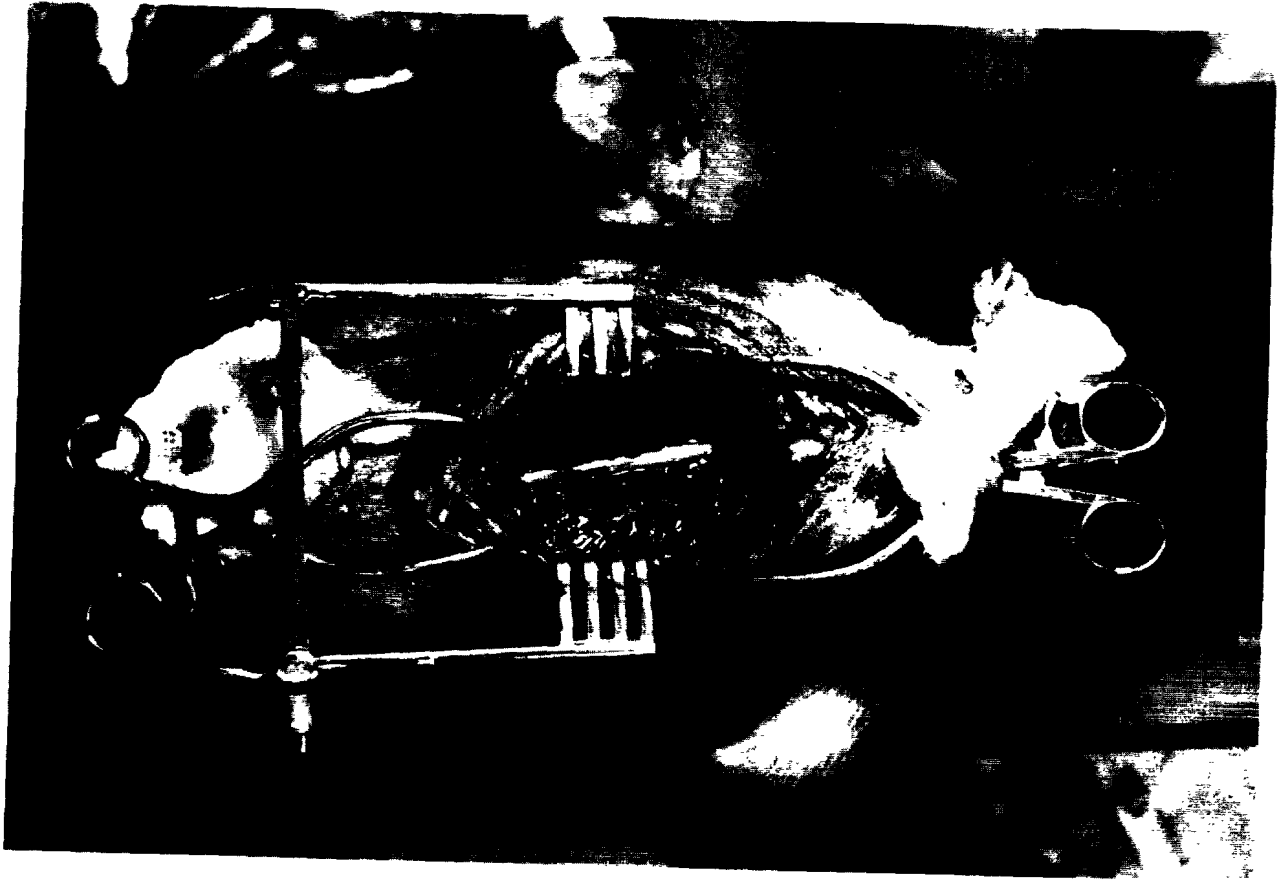


Fig. 1 Dog after laminectomy showing the exposed spinal cord.

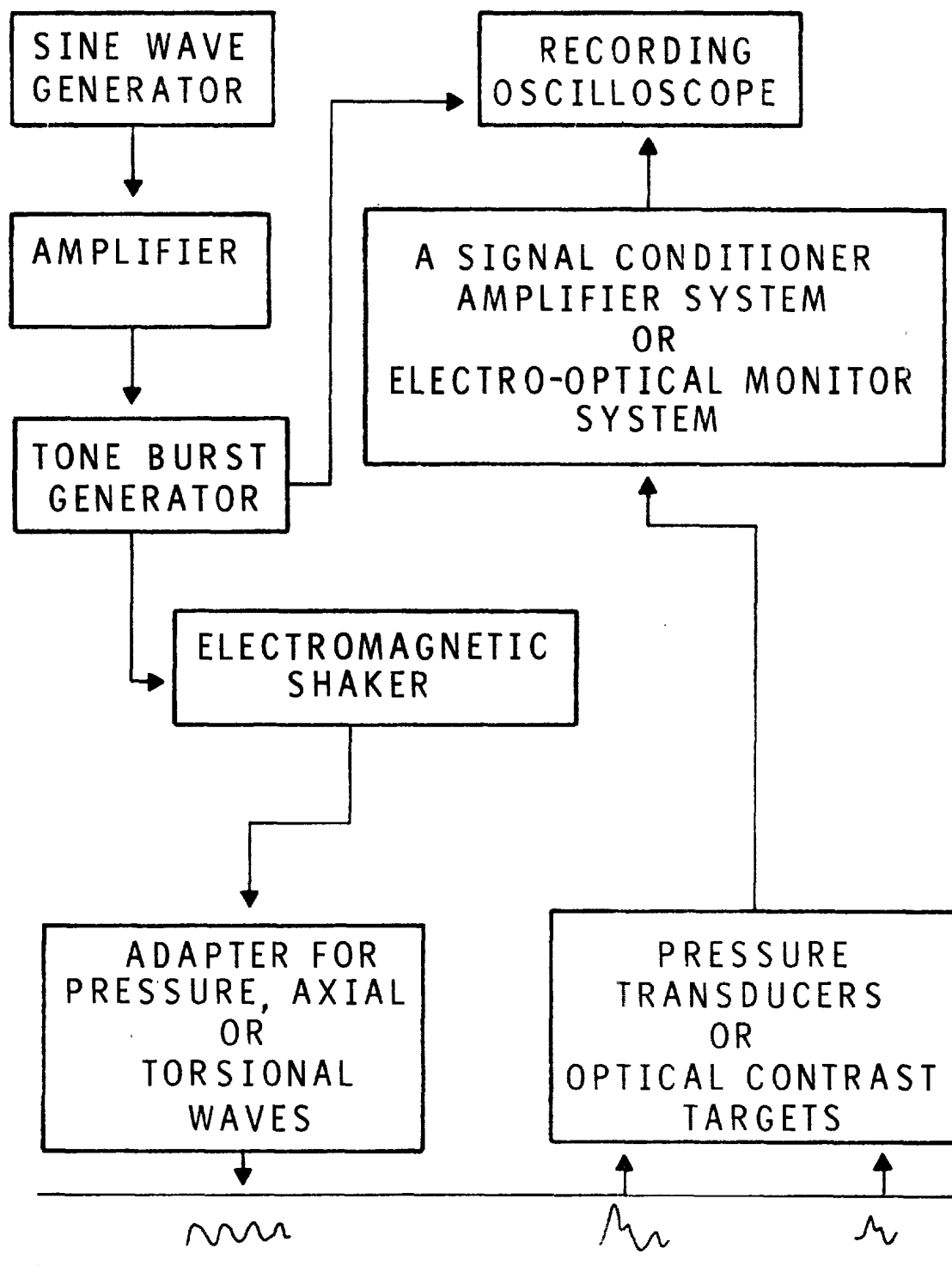


Fig. 2 Schematic of the experimental set up to induce and monitor waves on the spinal cord.

in Fig. 3. The signals obtained were recorded on the oscilloscope and a Polaroid picture taken for later analysis and data reduction. Typical pressure wave recordings thus obtained are shown in Fig. 4.

In the contract proposal, we had intended to determine the logarithmic decrement of the pressure wave by positioning the second transducer at various distances from the first transducer and monitoring the pressure waves. A plot of the amplitude ratio as a function of distance would have yielded some data on the dissipative properties of the dura mater. However, it was not possible to determine the true amplitude ratio of the pressure waves between the two locations with the present method of monitoring the pressure waves. This was due to the fact that the Entran pressure transducers mounted on probes had to be pressed against the cord to pick up the signal and the amplitude of the pressure waves picked up was highly dependent on the proper positioning and preload given to the transducer. To estimate the preload in the present system would have required mounting a LVDT in series with the pressure probe. To overcome this difficulty without additional equipment purchase, we tried a different system using Statham P23db blood pressure transducers. A fine 22 G hypodermic needle, connected to a flexible tubing, was attached to the transducer and the needle was inserted into the subarachnoid space to measure directly the pressure waves of the CSF. However, in trying out this procedure (on three dogs) we encountered considerable difficulties. Statham dome type pressure transducers are very poor in performance for frequencies above 10 Hz because of the distensibility of the fluid-filled flexible tubing between the needle and the transducers. At higher frequencies, we could definitely observe the whipping action on the flexible tubing resulting in erratic signals. Geddes (1970) has analyzed and shown that the frequency response for these transducers become nonlinear above 40 Hz with a resonance frequency of 280 Hz. After these trials, we are convinced that the only way to measure pressure is to insert a micro-tip pressure transducer, such as the one manufactured by Millar, directly into the subarachnoid space of the spinal cord. This could be a worthwhile point to pursue in a future investigation. Due to the unavailability of such transducers in our lab, we did not attempt to evaluate the logarithmic decrement in the pressure wave propagation studies of the spinal cord.

(b) Axial and torsional waves:

Even though not specifically included in the present contract proposal, the experiments on axial and torsional waves were also undertaken with the aid of an Optron Electro-optical Tracker System (model 810) which was purchased for our laboratory through NIH funding. To induce the axial and torsional waves, a special adapter shown in Fig. 5, was designed and attached to the electromagnetic shaker. The design of the adapter was similar to the one described by Moritz (1969) in his study of waves in arteries. The lower portion of the Plexiglass adapter was attached to the dura mater of the spinal cord and the vibrator probe connected to the adapter to induce torsional and axial motions respectively.

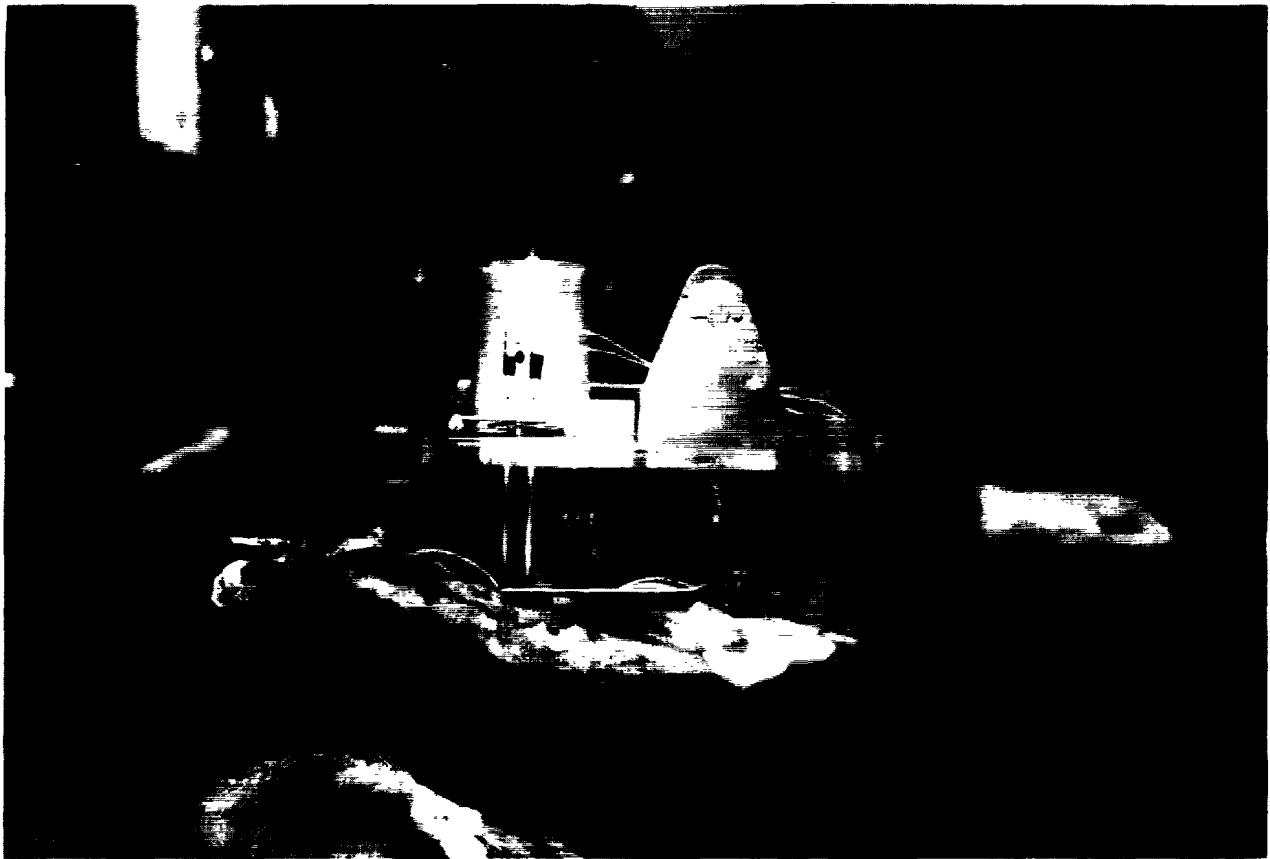
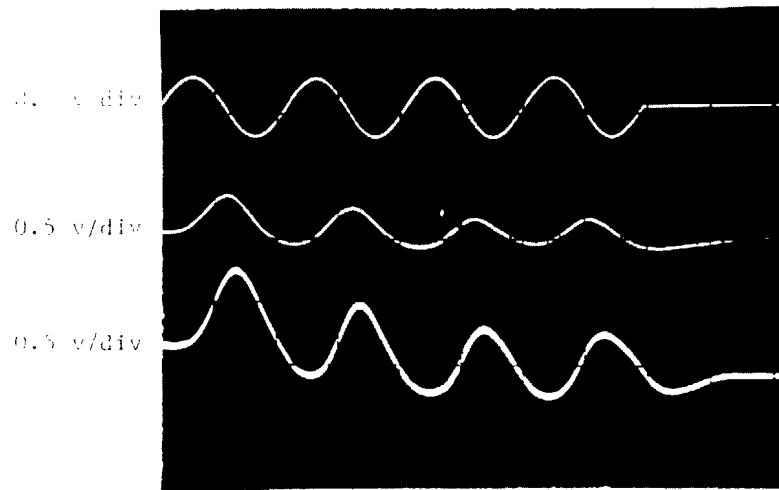
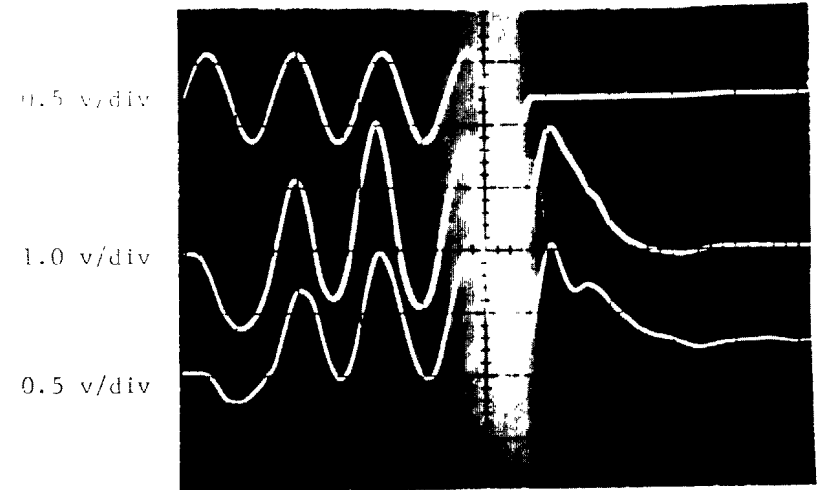


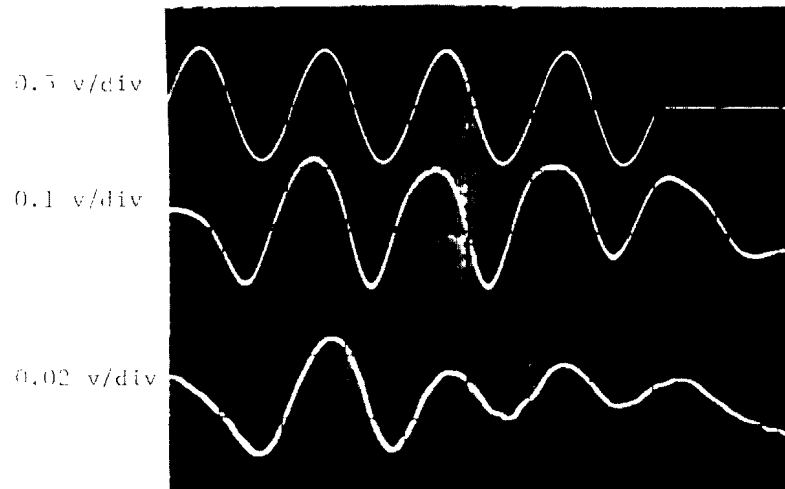
Fig. 3 Set up of the vibrator and pressure transducers mounted on a stand to measure the pressure wave propagation.



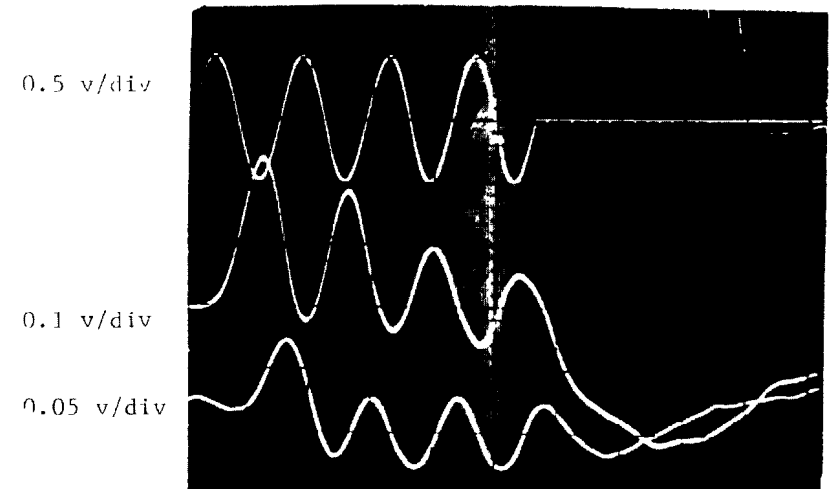
Frequency 100 Hz: 5 msec/div



Frequency 140 Hz: 5 msec/div



Frequency 240 Hz: 2 msec/div



Frequency 340 Hz: 2 msec/div

Fig. 4 Recordings of pressure waves (top signal is the input, the middle signal is picked up by the proximal transducer and the bottom signal is picked up by the distal transducer. The sensitivities and the time scale setting of the scope are indicated on the side of the Figure).



Fig. 5 Adapter attached to the electromagnetic vibrator to induce torsional and axial waves.

Two small targets (0.65 cm. dia.) made of plastic tape with an optical discontinuity (black and yellow interface) were glued with cyanoacrylate to the surface of the exposed dura, which was pre-cleaned with acetone. Regulated D-C light sources illuminated the targets and the optical head of the electro-optical tracker (one for each target) were focussed on the targets. Light was reflected from the surface of the target and focused, by means of a lens system, upon the photo-sensitive cathode of the photo-multiplier tube. A secondary emission of electrons, thus produced, is accelerated down the tube towards the defining aperture which sees only a very small part of the electron image. The deflection oscillator causes the beam of electrons to sweep back and forth across the aperture. As the line of contrast sweeps past the aperture, there is a sharp jump in output current. The logic circuitry then converts this to a voltage proportional to the position of the interface on that sweep. A high scanning rate of 50 kHz provides for a very high frequency response. The propagating wave was sensed by electro-optical trackers at two different sites and were again displayed on the storage oscilloscope and photographed for later analysis. The distance between the targets for each experiment was then directly measured on the spinal cord. The set up for torsional waves is shown in Fig. 6. Typical axial and torsional signals obtained are shown in Figs. 7 and 8 respectively. At the end of these experiments, the diameter of the cord was measured with precision calipers. After sacrifice, the dura was dissected out and its thickness measured.

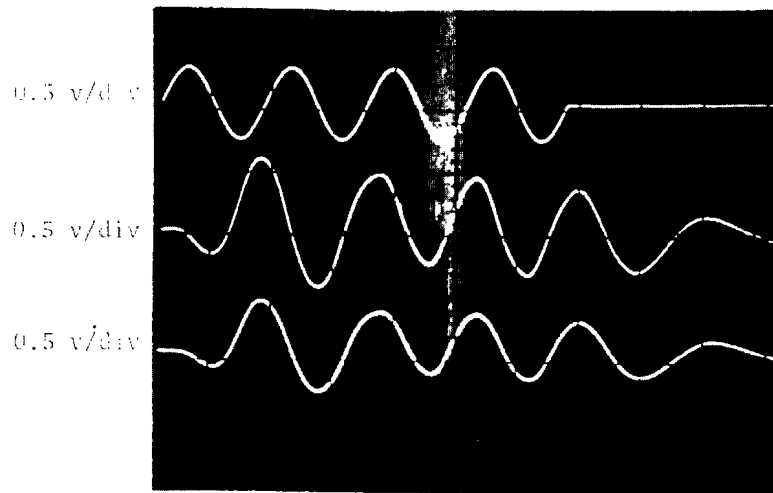
3. Data Reduction and Error Analysis

To determine the wave speeds on the three types of waves, the data reduction consisted of: (1) measuring the distance, Δx , between the pressure transducers for pressure waves or between the targets for axial and torsional waves and (2) determining the time lag, Δt , between the two signals from the Polaroid pictures of the traces recorded on the oscilloscope. In the case of pressure waves, the distance, Δx , between the two transducers was directly read from the specially constructed stand. For the other two waves, the distance between the targets mounted on the cord was directly measured using a precision caliper. The possible errors involved in these measurements as well as the technique used in the determination of the time lag, Δt , will be discussed at the end of this section.

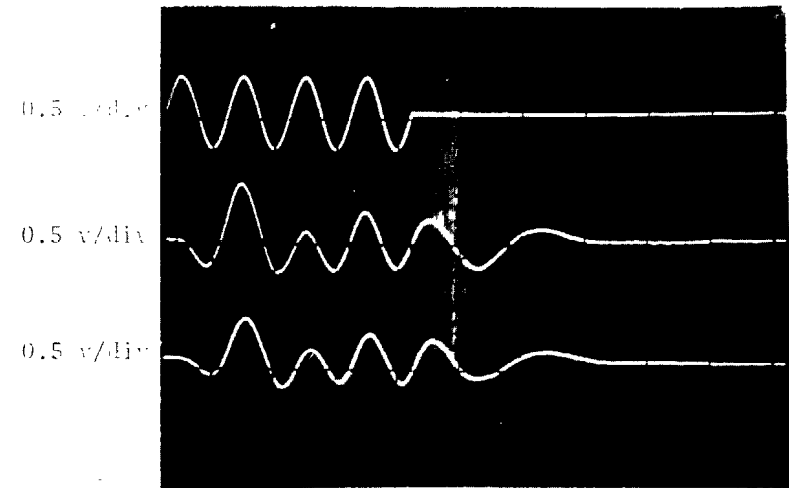
The determination of the time lag, Δt , between the two photographed signals stored in the oscilloscope, used a method similar to that described by Van Buskirk (1970). The scheme describing the method is illustrated in Fig. 9. Essentially the method utilizes the intersections of the tangents at two successive inflection points to determine the time difference, Δt . Several measurements can be taken on successive "apparent" inflection points and the average taken as the time lag for computations. However, because the total length of the exposed spinal cord was always less than 10 cm, and since the distance between the targets was restricted by attenuation to about 4 cm or less, the time lag between



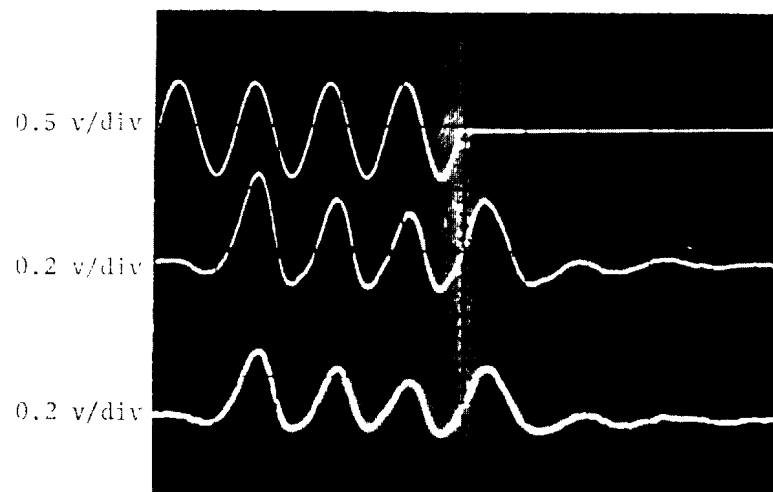
Fig. 6 Optron electro-optical tracker system for monitoring the torsional waves.



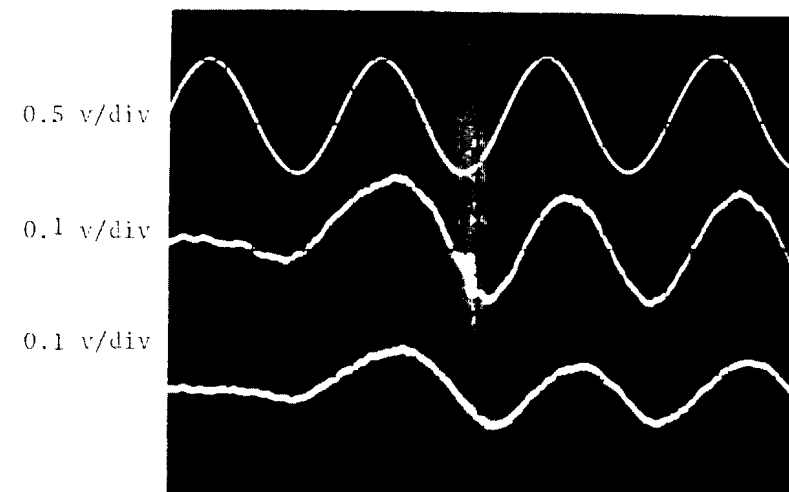
Frequency 60 Hz: 10 msec/div



Frequency 100 Hz: 10 msec/div



Frequency 100 Hz: 10 msec/div



Frequency 180 Hz: 2 msec/div

Fig. 7 Recording of axial waves (top signal is the input, the middle signal is picked up by the proximal target and the bottom signal is picked up by the distal target. The sensitivities and the time scale setting of the scope are indicated on the side of the Figure).

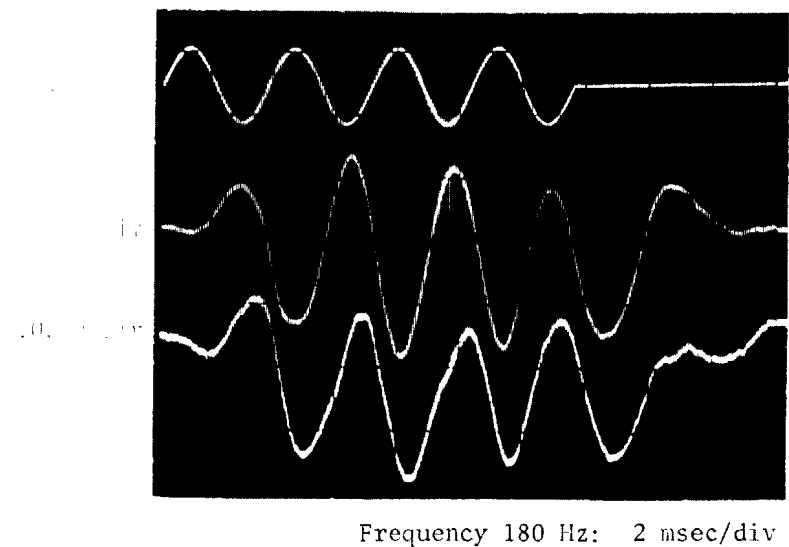
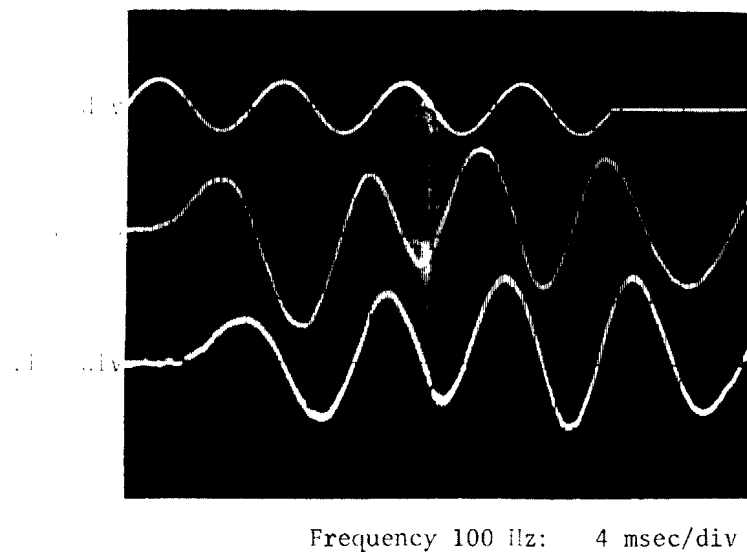
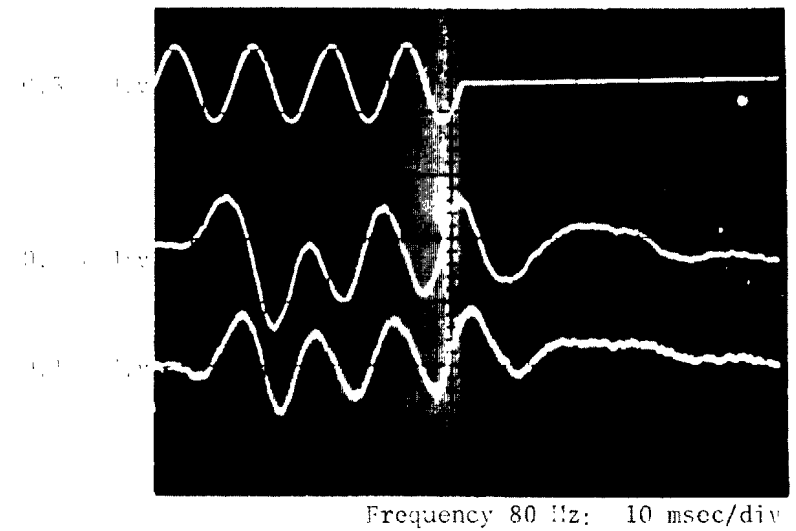
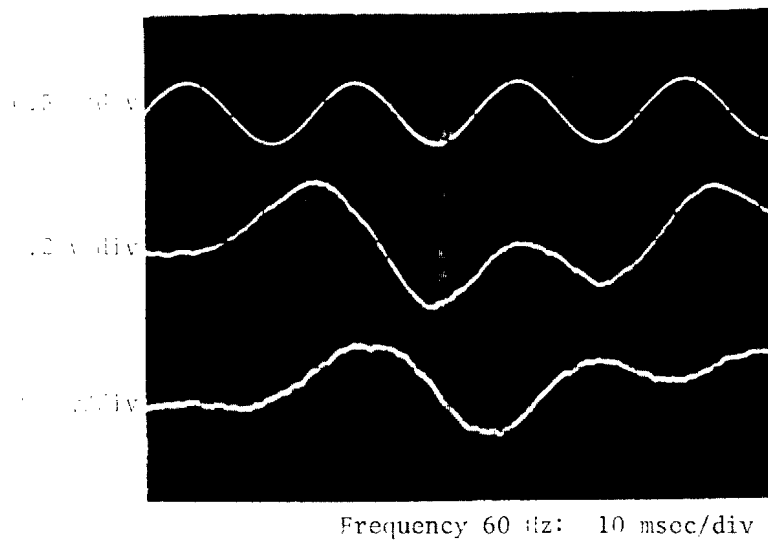


Fig. 8 Recordings of torsional waves (top signal is the input, the middle signal is picked up by the proximal target and the bottom signal is picked up by the distal target. The sensitivities and the time scale setting of the scope are indicated on the side of the Figure).

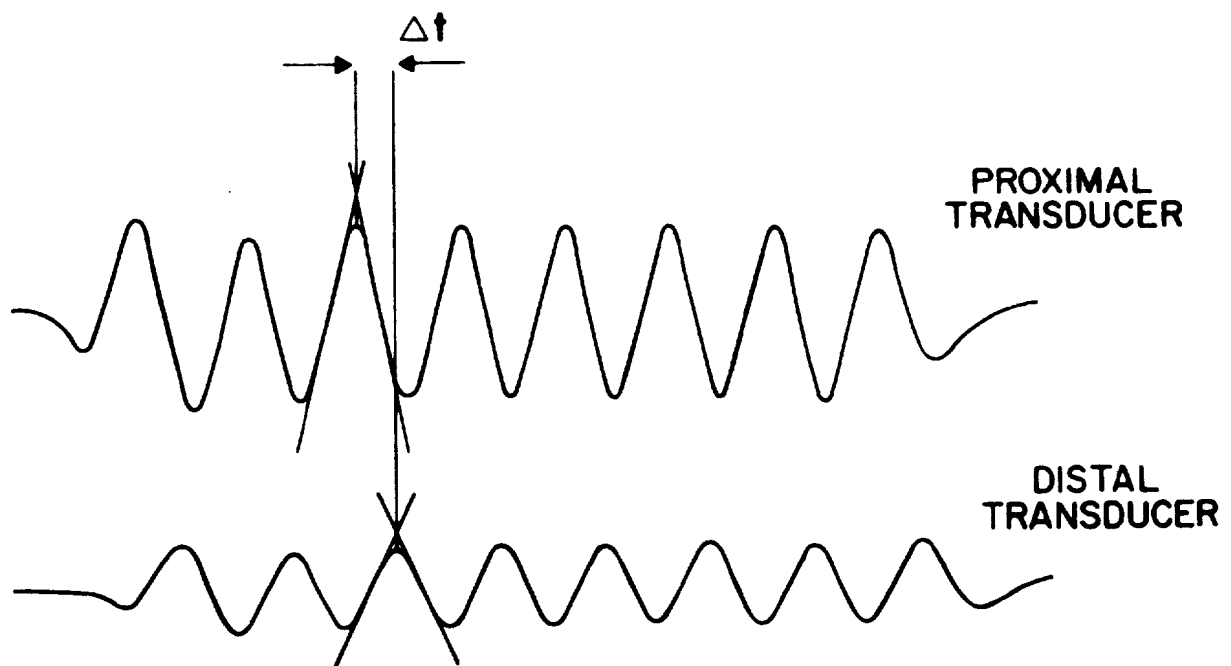


Fig. 9 Schematic of the time lag measurement.

the signals were of the order of 1 msec. It will be very difficult to manually measure such time lags without introducing substantial errors. Hence, the data reduction was performed on a digitizer connected to a Hewlett-Packard Model 9820 programmable calculator. A specific computer program was written for this data reduction. Initially, the photograph was aligned with the XY axes of the digitizer and a scale factor was determined to relate the time scale of the photograph to the coordinates of the digitizer. The tangents at the inflection points were drawn by tracing the straight line portion of the "sinusoidal" signal with the digitizer probe and a straight line was fitted using a least squares criterion. The program is then used to calculate the intercepts of straight lines of the inflection points. To determine the lag between the two signals, the calculator prints out the time difference between the interception points. The computer program listing is given in Appendix A.

With the expected errors in Δx and Δt thus established, the maximum expected error in the phase velocity c can be estimated. Since c is given by

$$c = \Delta x / \Delta t$$

the maximum expected relative error is given by

$$\delta c / c = \delta(\Delta x) / \Delta x + \delta(\Delta t) / \Delta t$$

where $\delta(\Delta x)$ and $\delta(\Delta t)$ are the maximum expected errors in the measurement of Δx and Δt .

In the measurement of the distance between the targets, the maximum expected error can be estimated for the different types of waves. In the case of the pressure waves, the distance between the transducer probes are directly measured on the scale fitted to the specially constructed stand. However, in taking this value for the measurement of Δx , it is assumed that the transducer probes are parallel to each other where it is touching the spinal cord. This assumption was checked by actually measuring the distance between the probes at that level after the experiment and comparing it with the readings obtained from the scale. The maximum difference observed between the two measurements were 1 mm in 20 mm or 5%.

In the case of axial waves, the distance between the targets were directly measured using a vernier caliper. Assuming the maximum error in this measurement to be 1 division in the main scale of 1 mm in target distances of the order of 40 mm, the error in measurement of Δx in axial waves is estimated to be 2.5%.

In the case of torsional waves, the target distance Δx was similarly measured using the caliper. However, the finite dimensions of the targets caused some uncertainty as to the definition of Δx since the point on the line of contrast viewed by the trackers could not be exactly identified. The lines of contrast of the targets were about 6 mm long and assuming that the point in the line of contrast can vary by as much as 3 mm in target

distances of the order of 20 mm, errors as much as 15% can be expected. But this error was kept to a minimum by taking care to keep the optical trackers focused on the centers of the target lines.

The program written for the digitizer to determine the time lag between the signals was tested on photographs of pure sinusoidal signals with known time lags. The accuracy of the measurement of the time lag with the procedure described above was found to be within 0.5% when the time lag was 5 msec. However, due to the restrictions on targets distances to within 4 cm, the typical time lags were of the order of 1 msec. Since there was no way to compare the measured time lags with any known values for the recorded data, the measurements on the same photograph were repeated several times to determine the variations in time lag values. In this manner, a conservative error estimate of 15% in time lag measurement was obtained.

4. Computation of Elastic Moduli

Having computed the wave speeds, the corresponding elastic moduli were easily found from the relations given in eqs. (1) - (3). For the case of the pressure waves, two additional measurements of the radius of the cord and the thickness of the dura mater are necessary. These diameter measurements were made in situ at the end of the experiment as soon as the dog was sacrificed. The thickness was measured in vitro by cutting out a segment of the cord. Several measurements of the radius and thickness were made and an average value is computed for each dog. Also, in the case of the pressure waves, the density of the CSF was taken as 1.0 gm/cm^3 . The values for the Poisson's ratio and the density of the dura mater required for the other two waves were obtained from those reported in the literature (see Clauser et al. 1969). The values used were 1.1 gms/cm^3 for density and 0.5 for the Poisson's ratio.

5. Results and Discussion

After preliminary trials on 4 dogs in which the logistics of the experiment were worked out and a method of procedure established, a total of 10 dogs were used in measuring all the three types of waves. The frequency of the input sine wave was varied from 40 Hz to approximately 300 Hz. Below 40 Hz, the signals exhibited interference patterns which were probably due to reflections, i.e., the peaks and valleys of the monitored signals were not well defined. Even though measurements were carried out to as high as 600 Hz in some experiments, it was noticed that at higher frequencies, the spinal cord began to respond to a 4 cycle input as a single burst. The frequency resolution became a function of total duration of the gated signal rather than the signal itself. Of the three types of waves, the torsional waves exhibited the slowest wave speed and highest dissipation. Thus, the distance between the targets in torsional wave measurement was set to less than 1.5 cm. The range of frequency response was generally limited to 40-180 Hz. The axial waves were the fastest and to insure successful measurements of the wave speed, the targets had to be placed at least 4 cm. apart.

Fig. 10 shows the wave speed as a function of frequency of the pressure waves measured. At each frequency, the mean and standard deviation of several measurements from the 10 experiments were computed and plotted. The wave speed for the pressure measurement was in the order of 25 m/sec. Fig. 11 shows a similar variation of the Young's modulus found through eq. (1) as a function of frequency. The Young's modulus thus obtained is of the order of 2×10^8 dynes/cm². Table 1 shows the wave speed and the Young's modulus at various frequencies along with the standard deviation. At each frequency, the number of measurements out of which the average value was obtained is also indicated in the Table.

Figs. 12 and 13 show the variation of the torsional wave speed and the shear modulus as a function of frequency and the results have also been tabulated in Table 2. Similar results for the axial wave experiments are given in Figs. 14 and 15 and Table 3.

Even though a total of 10 dogs were used in this series of experiments, not all the measurements were successful. Of the three types of waves, the torsional waves were the slowest and were most successfully measured with the target distance of about 1.5 to 2 cm.

The measurement of pressure waves depended crucially on the positioning and the pre-load on the transducers. Sometimes, while inducing the pressure waves, the spinal cord tended to slip out from under the pressure transducer and thus yielded inconsistent signals. In one of the experiments, the dog died during the pressure wave measurements and the wave speed increased at least by an order of magnitude. These particular measurements were excluded from the final analysis.

The axial wave speed was the fastest of the three waves and necessitated the targets to be mounted far apart from each other. For target placements 4 cm from each other, we detected clear signals from both the targets. However, the time lag between the signals was of the order of 0.2 msecs. and measurements of such small times were very difficult even with the help of the digitizer. We tried placing the targets 7 cm. apart and were not successful in getting any measurement with the distal target due to the attenuation. In spite of very careful measurements, our results from several trials were very inconsistent and hence our reported results on the axial wave speed and the computed Young's modulus are tentative. A different approach, perhaps using tape recordings of the signals and computer analysis is required to accurately determine the time lags in axial wave signals.

Even though some variations of wave speed were observed with frequency, a definite trend in either increase or decrease in wave speed was undetectable with the limited number of measurements.

On each of the type of waves, assuming the spinal cord is mildly dispersive, a straight line was fitted to the values at various frequencies using a least square fit. The area under this straight line, bounded by the x axis was computed and using a rectangle of the same area, a mean

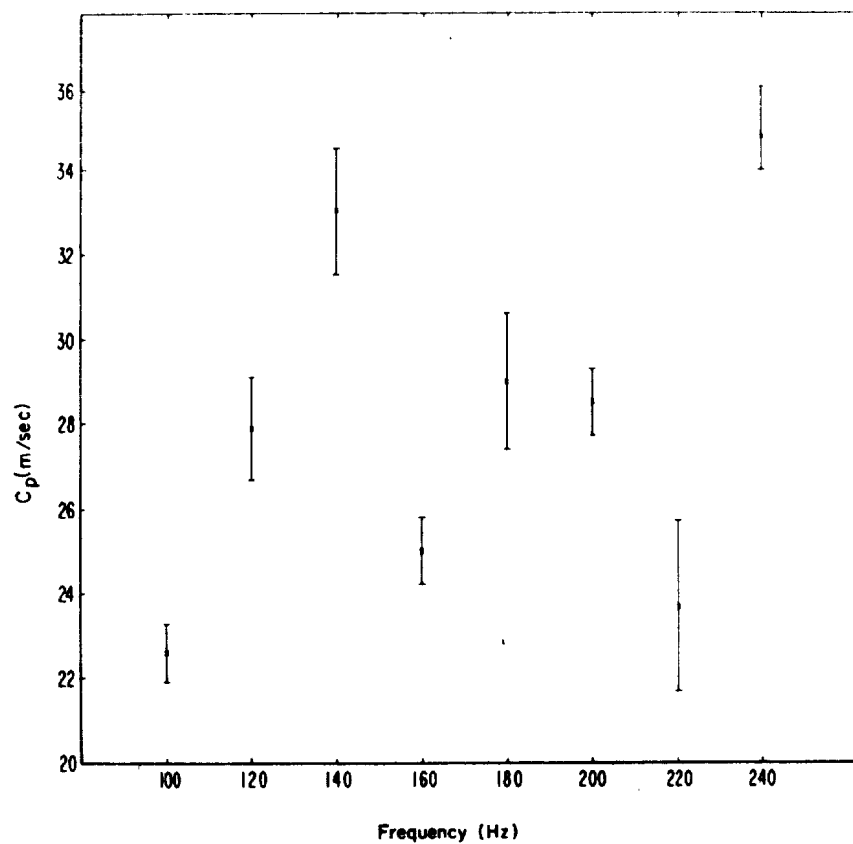


Fig. 10 Wave speed as a function of frequency for pressure waves.

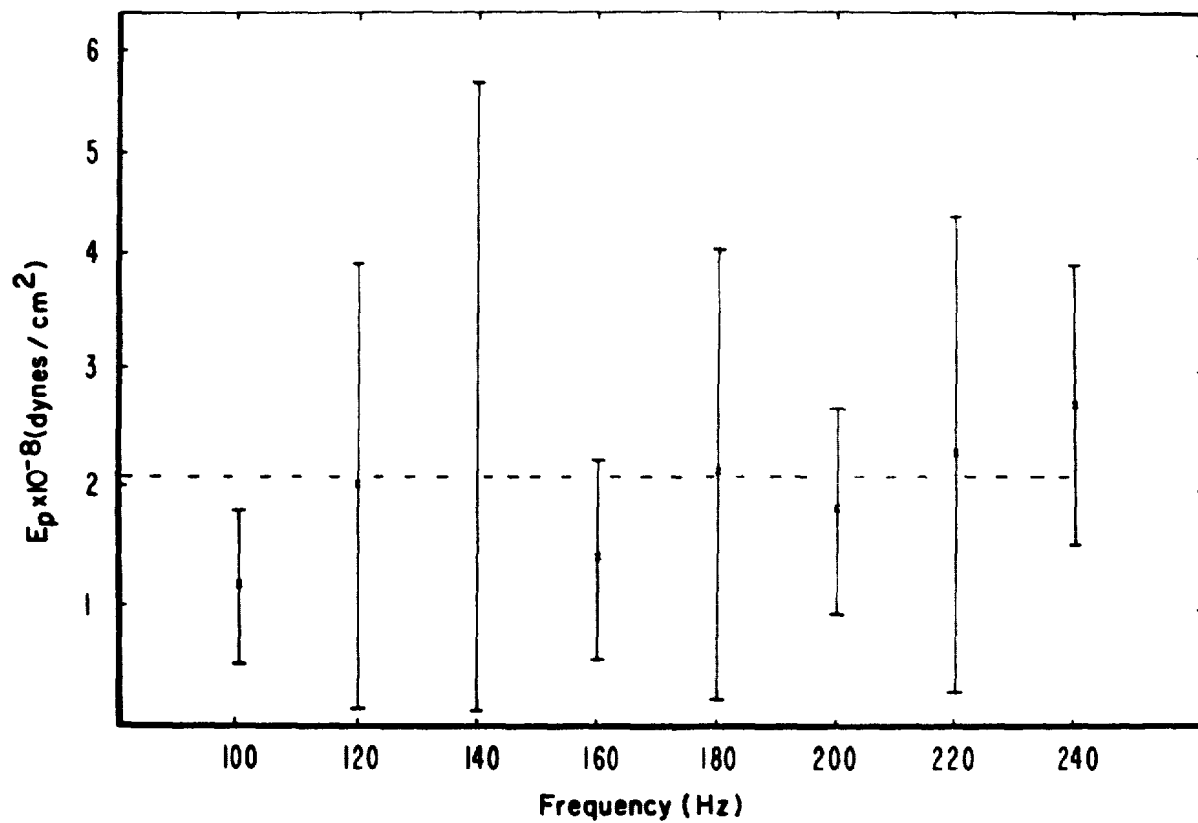


Fig. 11 Young's modulus, E_p , as a function of frequency for pressure waves.

Frequency Hz	No. of trials	Wave Speed m/sec (\pm SD)	$E_p \times 10^{-7}$ dynes/cm ² (\pm SD)
100	8	22.60 (7.36)	11.80(7.95)
120	6	27.94 (12.96)	20.28(19.20)
140	5	33.38 (15.61)	27.95(26.37)
160	5	24.96 (8.83)	14.19(8.60)
180	6	29.43 (16.06)	21.16(19.20)
200	5	28.56 (7.92)	18.51(9.07)
220	7	28.88 (14.29)	23.77(20.03)
240	6	34.93 (10.66)	27.14(12.11)

Table 1. Pressure Wave Speed (\pm Standard Deviation) and the Young's Modulus (\pm SD) for various frequencies.

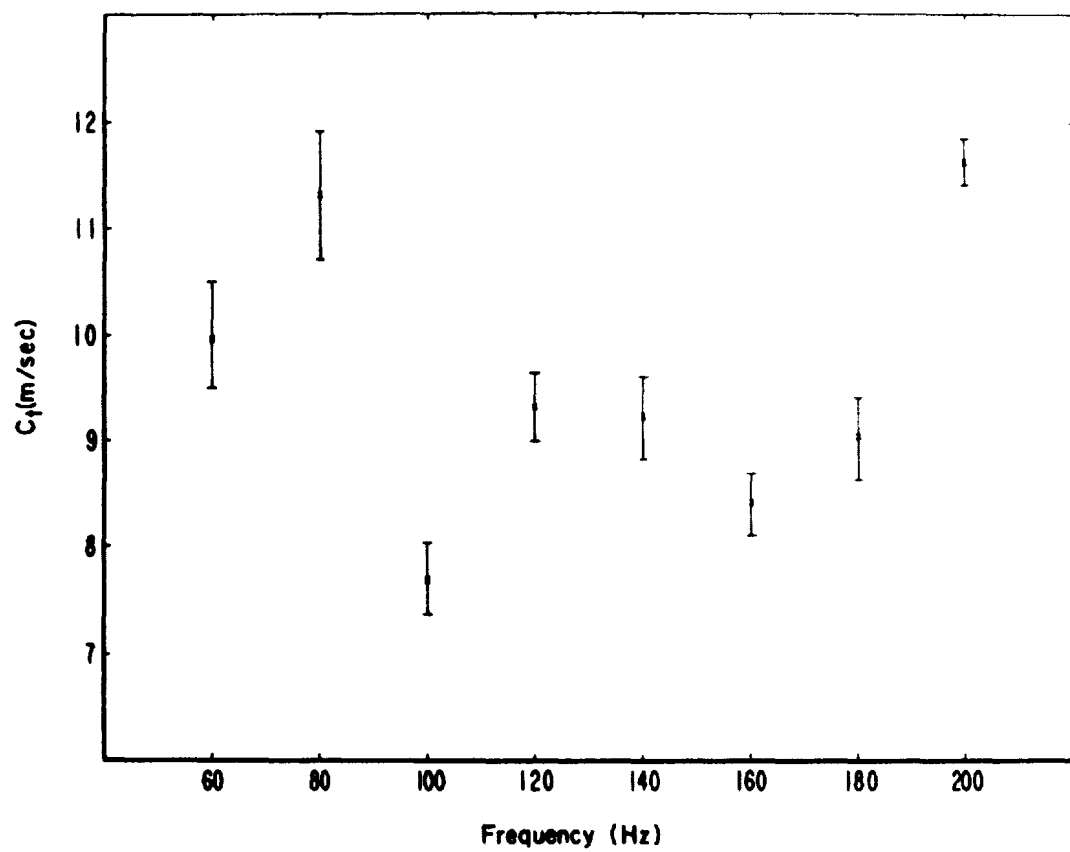


Fig. 12 Wave speed as a function of frequency for torsional waves.

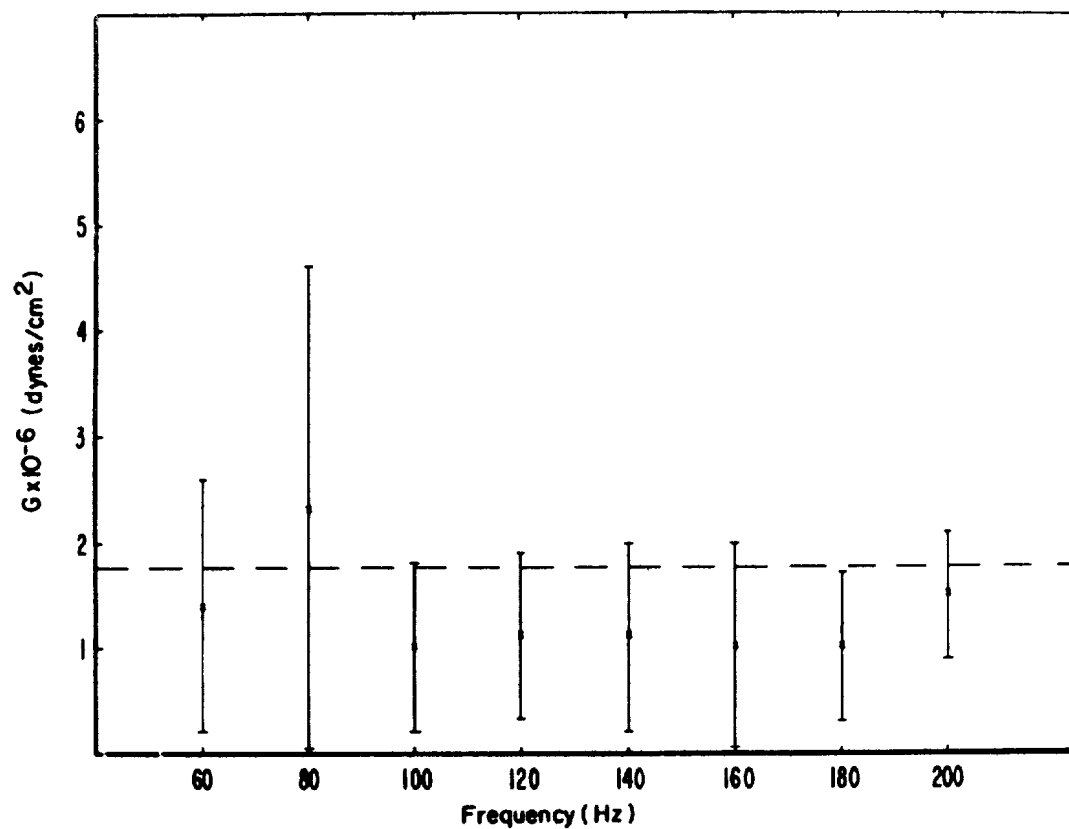


Fig. 13 Shear modulus, G , as a function of frequency for torsional waves.

Frequency Hz	No. of trails	Wave Speed m/sec (\pm SD)	Shear Modulus $G \times 10^{-6}$ dynes/cm ² (\pm SD)
60	5	9.97(5.11)	1.40(1.24)
80	9	11.32(6.38)	2.32(2.27)
100	10	7.70(3.15)	1.05(0.36)
120	7	9.30(3.32)	1.14(0.83)
140	5	9.24(3.95)	1.13(0.99)
160	5	8.42(3.08)	1.00(0.98)
180	5	9.12(3.99)	1.04(0.69)
200	3	11.63(2.40)	1.53(0.63)

Table 2. Torsional Wave Speed and the Shear Modulus for various frequencies.

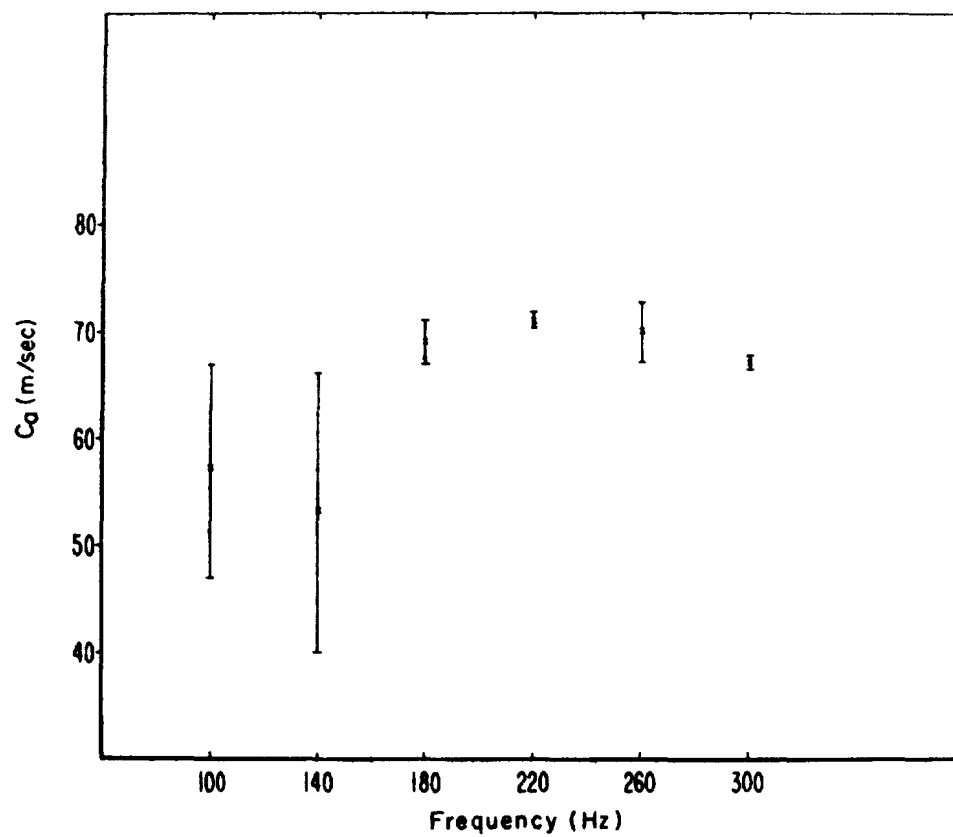


Fig. 14 Wave speed as a function of frequency for axial waves.

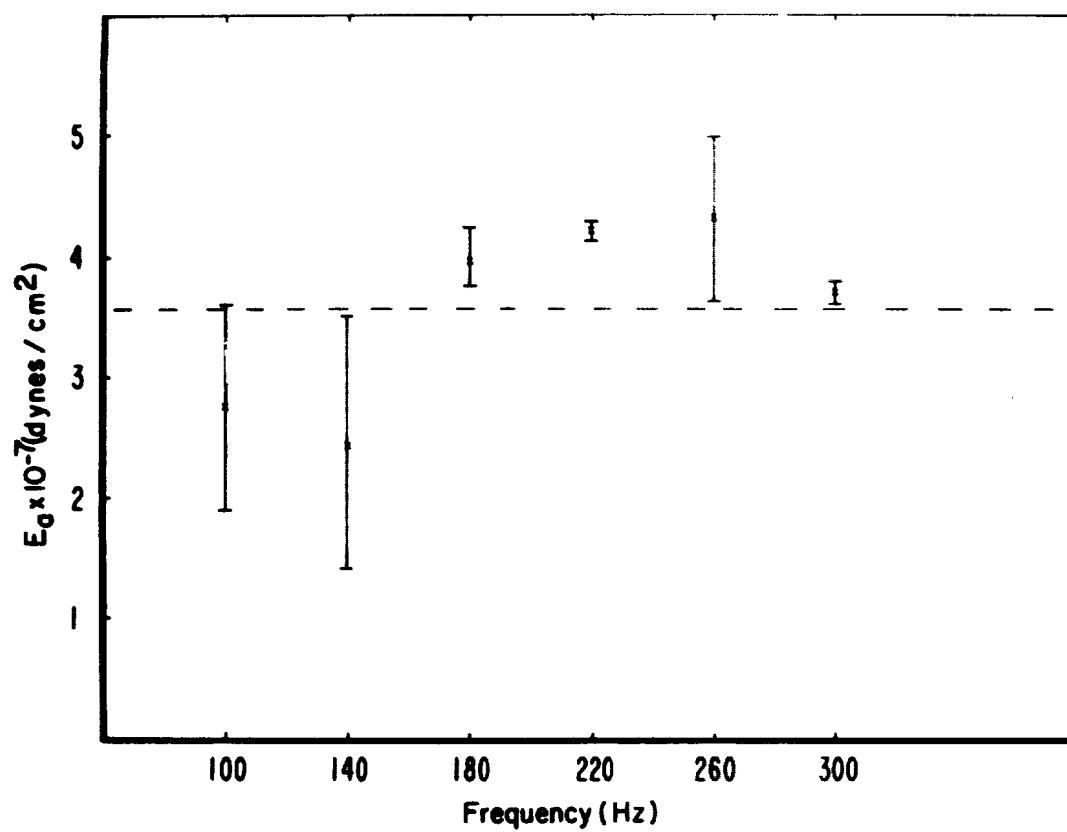


Fig. 15 Young's modulus, E_a , as a function of frequency for axial waves.

Frequency Hz	No. of trials	Wave Speed m/sec (\pm SD)	$E_a \times 10^{-7}$ dynes/cm ² (\pm SD)
100	4	57.16(10.02)	2.76(0.90)
140	2	53.42(13.47)	2.43(1.19)
180	2	69.28(2.14)	3.96(0.25)
220	2	71.49(0.80)	4.22(0.09)
260	2	70.34(3.23)	4.31(0.69)
300	2	67.23(0.43)	3.73(0.05)

Table 3. Axial Wave Speed and Young's Modulus for various frequencies.

value for the elastic moduli applicable at all the frequencies were obtained. These values have been indicated by the dotted horizontal lines in Figs. 11, 13 and 15. These values are

$$E_p = 2.060 \times 10^8 \text{ dynes/cm}^2 \text{ (3181 psi)}$$

$$G = 1.762 \times 10^6 \text{ dynes/cm}^2 \text{ (25.56 psi)}$$

$$E_a = 3.567 \times 10^7 \text{ dynes/cm}^2 \text{ (517 psi)}$$

McElhaney et al. (1973) performed in vitro tensile tests on excised dura mater from the head of cadavers and rhesus monkeys and reported mean values for the Young's modulus of 6000 psi increasing to a value of 8800 psi at a strain rate of 6.66 sec^{-1} . By comparison, our in vivo study in the canine spinal cord yielded a mean value of 3180 psi for the circumferential Young's modulus with the pressure wave study and 517 psi for the axial Young's modulus from the axial wave study. The shear modulus obtained from the torsional wave propagation study yielded a mean value of 25 psi and, as far as we are aware, no data has been reported in the literature to compare our results with.

McElhaney et al. (1973) have pointed out that microstructurally, the dura mater, in regions relatively free from large blood vessels, appeared to be a membrane with evident directions of fiber reinforcement. Their tensile tests were performed in three different directions, i.e., parallel, perpendicular and diagonal to the sagittal plane. However, their tests were inconclusive on the effect of fiber directions although a trend towards an increased modulus along the fiber direction was observed.

Our in vivo study, using three types of wave propagation, showed that the elastic modulus changes with direction. The spinal cord dura mater is not isotropic but has at least transversely isotropic material properties. Our results further indicate that the dura mater is strongest when loaded perpendicularly to its surface, i.e., resulting in a predominant hoop stress and weakest when rotated, i.e., when significant shear stress is induced.

SUMMARY AND RECOMMENDATION

In this study, a series of experiments were conducted to determine the in vivo material properties of the spinal cord through its wave propagation characteristics. The results showed that the dura mater exhibited anisotropic material properties: being stiffest for loading normal to its surface and weakest when twisted. The limited number of measurements done in 10 dogs showed a large scatter in the data for elastic moduli. However, specific mean values for the Young's moduli in the circumferential and axial directions and a value for the shear modulus have been obtained. Such an order-of-magnitude result is already adequate for any mathematical modeling effort.

Specific recommendations for refining the obtained results are given below.

- (1) More experiments need to be done to obtain statistically significant values for the elastic moduli of the spinal cord.
- (2) Microcatheter-tipped pressure transducers need to be used to avoid the difficulties described in using the dome-type strain gage transducers in the pressure-wave study. The use of microtipped-transducers would also help in estimating the damping of the pressure waves with distance.
- (3) For axial wave studies, recording the signals on tape for later computer analysis may be attempted to enable a more accurate measurement of the time lag.
- (4) The measurements on the three types of waves can be repeated after the dog is dead so that any necrotic changes in material properties can also be measured.
- (5) The measurements can be repeated with the CSF drained and the spinal nerve tethering removed. This is easily done by cutting the spinal nerves near its exit from the cord. The new data will give an estimate of the CSF contribution to wave propagation.
- (6) The dura can be dissected out and the wave propagation studies repeated on the pia mater.
- (7) The entire series could be repeated as a function of decreasing arterial blood pressure until death. For further comparison, the tissue could be fixed in formalin and the wave propagation measurements repeated in situ. Thus, the differences, if any, between in vivo, in situ and in vitro material properties can be delineated.

REFERENCES

1. Anliker, M. (1972), "Toward a Nontraumatic Study of the Circulatory System," Proc. Symp. on Biomech., Its Foundations and Objectives, Ed. Y. C. Fung, et al., Prentice Hall.
2. Atabek, H.B. (1968), "Wave Propagation Through a Viscous Fluid Contained in a Tethered Initially Stressed Orthotropic Elastic Tube," Biophys. J., 8, 626-649.
3. Breig, A. (1960), Biomechanics of the Central Nervous System, Almqvist and Wiksell, Stockholm, Sweden.
4. Clauser, C.E., Mc Conville, J.T. and Young, J.W. (1969), "Weight Volume and Center of Mass of Segments of the Human Body," AMRL-TR-69-70.
5. Fallenstein, G.T., Hulce, M.D. and Melvin, J.W. (1960), "Dynamic Mechanical Properties of Human Brain Tissue," J. Biomech., 2, 217-226.
6. Geddes, L.A. (1970), "The Direct and Indirect Measurement of Blood Pressure," Year Book Medical Publishers, Inc., Chicago, IL.
7. Klip, W., van Loon, P., and Klip, D.A. (1967), "Formulas for Phase Velocity and Damping of Logitudinal Waves in Thick-Walled Viscoelastic Tubes," J. Appl. Physics, 38, 3745-3755.
8. Liu, Y.K., Chandran, K.B. and Van Buskirk, W.C. (1974), "The In Vivo Dynamic Material Properties of the Canine Spinal Cord: A Feasibility Study," Final Report on Research Contract No. DAMD-17-74-G9384, U.S. Army Aeromedical Research Lab., Fort Rucker, Ala.
9. Maxwell, J.A. and Anliker, M. (1968), "Dissipation and Dispersion of Small Waves in Arteries and Veins with Viscoelastic Wall Properties," Biophys. J., 8, 920-950.
10. Moritz, W.E. (1969), "Transmission Characteristics of Distension, Torsion and Axial Waves in Arteries," Ph.D. Dissertation, Stanford University.
11. McElhaney, J.H., Melvin, J.W., Roberts, V.L. and Portnoy, H.D. (1973), "Dynamic Characteristics of the Tissue of the Head," Perspectives in Biomedical Engineering, Ed. R. M. Kenedi, MacMillan Press, London, 215-222.

12. Shuck, L.F. and Advani, S.H. (1972), "Rheological Response of Human Brain Tissue," Presented at the ASME Winter Annual Meeting, New York, N.Y., Nov., ASME Paper No. 72/WA BHF-2; J. Bas. Engng. ASME Trans. 94, Series D.
13. Van Buskirk, W.C., (1970), "Experimental and Theoretical Model Studies of Some Dynamic Response Characteristics of the Semi-circular Canals," Ph.D. Dissertation, Stanford University.
14. Womersley, J.R. (1957), "An Elastic Tube Theory of Pulse Transmission and Oscillatory Flow in Mammalian Arteries," WADC TR 56-614.

APPENDIX A

PROGRAM DESCRIPTION

For each sine wave on a photograph, we wish to determine three tangents, derive the abscissas of their points of intersection, P_1 , P_2 , and use these values to obtain the time lag between the second and third signals (see Figure A1). The algorithm was implemented on a Hewlett Packard Model 9820 Calculator with a Model 9864A Digitizer having a resolution of .01".

Since the data generated by the digitizer are in units of length, a scaling factor is required to convert from length to the desired units of time. After setting the digitizer origin and aligning the photograph, the scale factor is calculated:

$$B = \frac{A}{|x' - x''|}$$

where A is the time in milliseconds per division of the oscilloscope graticule (entered via keyboard) and x' , x'' are the end points of the interval (entered via single samples of digitizer). Any number which is printed out by the calculator is first multiplied by this conversion factor.

To obtain the best straight line approximation of the tangents, $y = a_1x + a_0$, we calculate the linear regression of y on x using data generated by the digitizer. From the theory,

$$a_0 = \frac{\sum y_i \sum x_i^2 - \sum x_i \sum x_i y_i}{n \sum x_i^2 - (\sum x_i)^2} = b \text{ (y intercept)}$$

$$a_1 = \frac{n \sum x_i y_i - \sum x_i \sum y_i}{n \sum x_i^2 - (\sum x_i)^2} = m \text{ (slope)}$$

The x_i , y_i are obtained by operating the digitizer in the continuous sample mode and utilizing a loop in the program to input the digitizer coordinates and accumulate the sums. The digitizer is moved slowly with a constant motion over the best straight line portion of the signal slope. To flag the program that the trace is completed, a single data entry is made below the origin.

After the coefficients for three tangents have been determined and printed out, the x coordinates of their points of intersection are derived. At point P_1 , the following relation holds:

$$m_1 x_1 + b_1 = m_2 x_1 + b_2$$

where b_1 , m_1 is the y intercept and slope of tangent t_1 and b_2 , m_2 is the y intercept and slope of tangent t_2 .

Using simple algebra,

$$x_1 = \frac{b_2 - b_1}{m_1 - m_2}$$

Similarly,

$$x_2 = \frac{b_3 - b_2}{m_2 - m_3}$$

These values are stored and printed out. Since the difference of these two values represent half the period of the signal, an approximate value of the signal frequency is also printed out.

When the third signal has been traced, two values of the time lag of the second signal to the third is calculated from the two peak positions of each signal.

If there is a prealigned plastic sheath for the photographs, the photograph alignment procedure can be eliminated. Also, if the photographs are the same size and the oscilloscope graticule is unchanged, the conversion factor is a constant and that procedure can be eliminated.

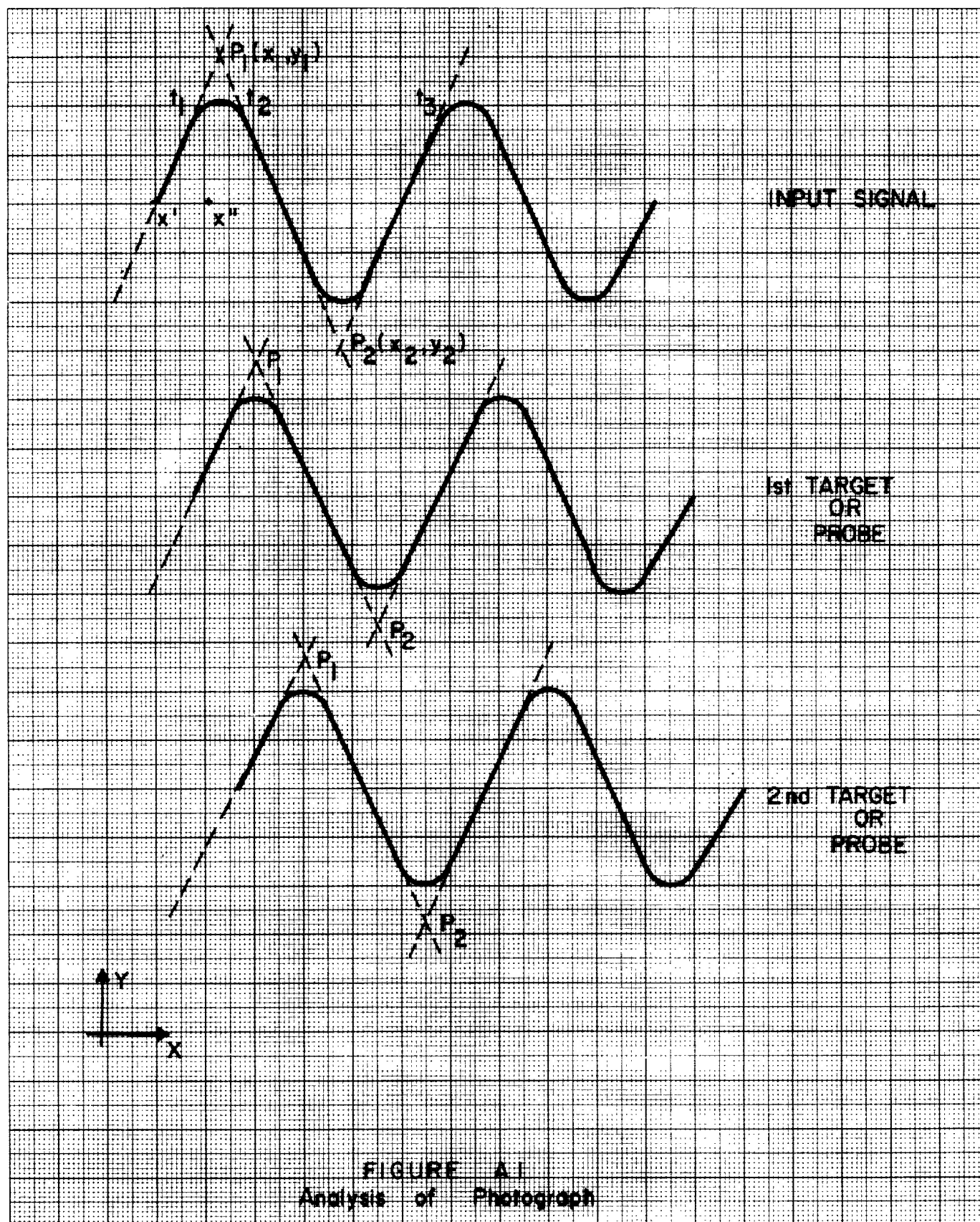


FIGURE A.1
Analysis of Photograph

PROGRAM FLOW

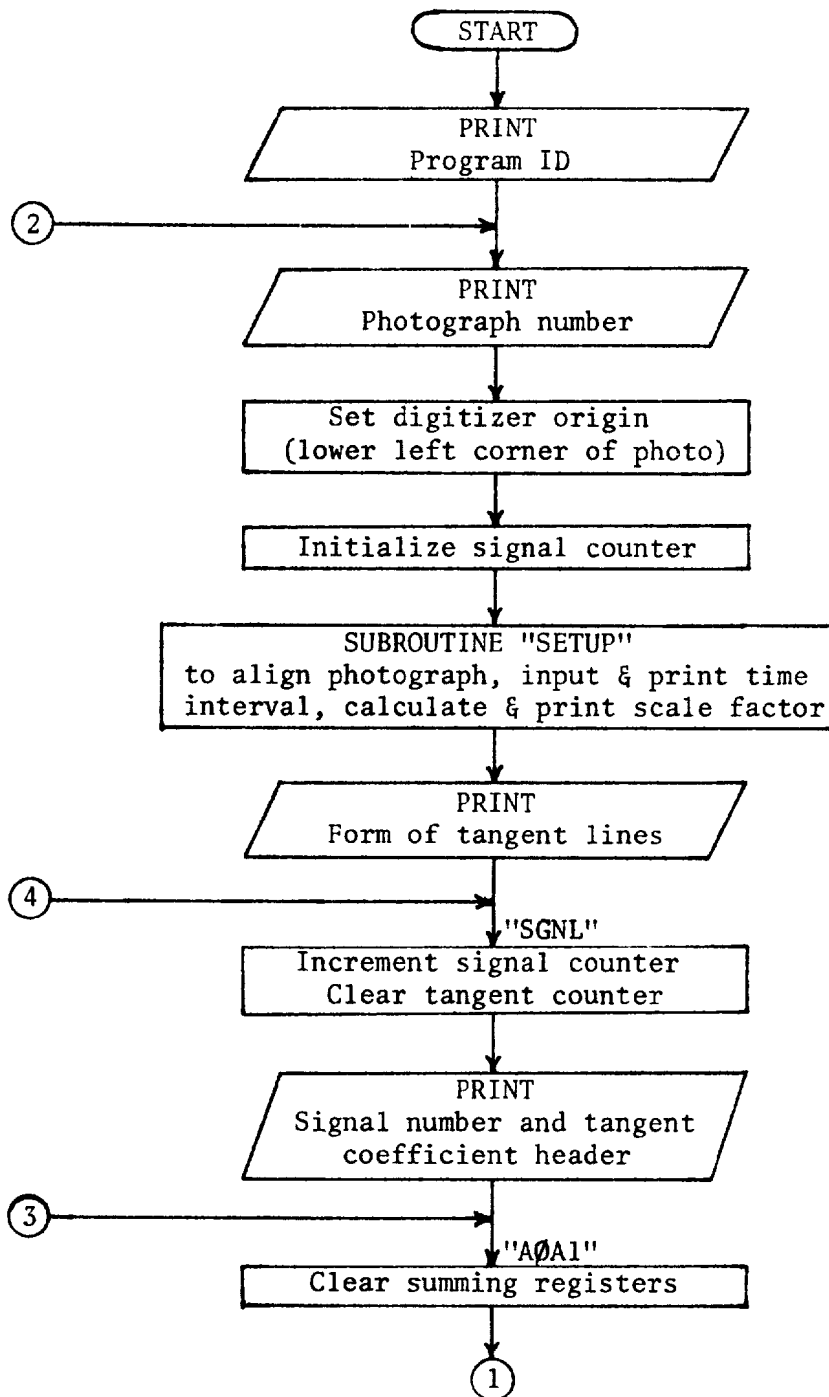


Fig. A2 Digitizer Program
Flow Chart

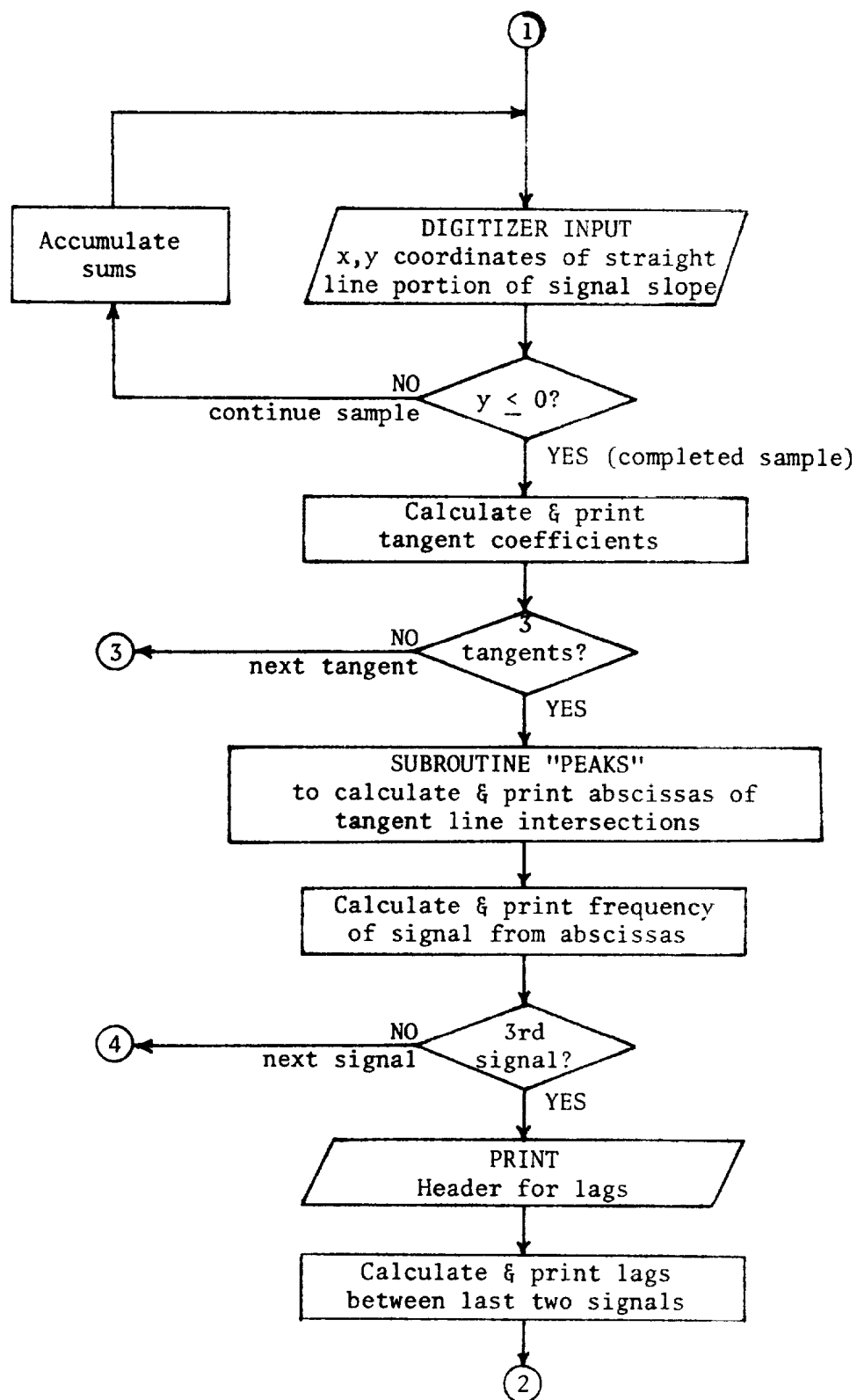


Fig. A2 Digitizer Program
(cont'd) Flow Chart

```

0:
END 3:PRT "PROGR
AM TO DIGI- ", "T
ZE SIN WAVES", "T
0 TRIANGLES 8"F
1:
PRT "GET PHASES"
1SPC 9F
2:
PRT "PHOTO NO.":
STP F
3:
SPC 2;WRT 9;ENT
"SET ORIGIN";CH
4:
0+Z;GSB "SETUP"F
5:
PRT " TANGENT LI
NES";"ARE OF THE
FORM";" Y = A0
+ A1*X";SPC 3F
6:
"SGNL";FXD 0;1+Z
+Z;0+AF
7:
PRT "*****SIGNAL
*****";Z;SPC 2F
8:
PRT " TANGENT
";" COEFFICIENT
S";SPC 2;FXD 3F
9:
"A0A1";0+C+R12+R
13+R14+R15+R16F
10:
RED 9;X;YF
11:
JMP 2*(Y<0.0)+1F
12:
C+1+C;R12+X+R12;
R13+Y+R13;X+R14
+R14;Y+R15+R15;
X+R16+R16F
13:
GTO -3F
14:
CR14-R12R12+R17F
5:
R10R14-R12R16;
R17+RA;(CR16-R12
R13)/R17+R(A+1)F
16:
PRT "A0=";RA;"A1
=";R(A+1);SPC 2;
2+A+AF
17:
IF A<4;GTO "A0A1
"F
18:
GSB "PEAKS"F
19:
SPC 3;PRT "FREQU
ENCY =";"(HZ.)";
1000/2B(R7-R6);
SPC 4F
20:
IF Z<2;GTO "SGNL
"F
21:
PRT "*****
*****";" LAGS
MSEC";"*****
*****"F
22:
SPC 2;PRT "LAG 1
=";B(R6-R8);"LA
G 2 =";B(R7-R9)F
23:
SPC 9;WRT 9;ENT
"NEXT PHOTO";CH
24:
GTO 2F
25:
"SETUP";WRT 9;
ENT "ALIGN PHOTO
";CH
26:
RED 9;X;Y;JMP 4+
Y>-1.0)+1F
27:
DSP Y;JMP 2*(Y<
1)-1F
28:
JMP 3*(Y>-1.1)-2F
29:
WRT 9;DSP Y;JMP
4+(Y=0.0)-3F
30:
WRT 9;DSP Y;WRT
9;GTO -4F
31:
WRT 9;ENT "TIME
INTERVAL?";A;
PRT "TIME INTERV
AL =";"(MSEC)";A
F
32:
WRT 9;ENT "PICK
INTERVAL";CH
33:
RED 9;X;Y;X+R0;
RED 9;X;Y;X+R1;
ABS (R0-R1)+C;A;
C+BF
34:
PRT "SCALE =";"(
MSEC/X)";B;SPC 5
F
35:
0+R0+R1F
36:
RET F
37:
"PEAKS";R6+R8;R7
+R9F
38:
(R0-R2)/(R3-R1)+
R6;(R2-R4)/(R5-R
3)+R7F
39:
JMP 2*(Z<1)+1F
40:
SPC 2;PRT "
PEAKS";SPC 2F
41:
PRT "NO. 1:";R6
;"NO. 2:";R7F
42:
RET F
43:
END F
R1289

```

Fig. A3 Digitizer Program Listing

REGISTER DEFINITIONS & USAGES

- A: (i) in subrouting "SETUP", used as an input register for keying in time interval of photograph.
- (ii) in main program, used as a counter for number of tangent lines.
- 0 - first incremented by 2 for each tangent. When
 - 2 - second >4 program jumps to subroutine "PEAKS".
 - 4 - third

Also, it is an index for storing y intercepts (a_0) & slopes (a_1) for tangent lines.

- B: inches \rightarrow millisecond conversion factor. Calculated in subroutine "SETUP".

X,Y: temporary coordinates of current point from digitizer.

- C: (i) in subrouting "SETUP", temporary storage for absolute value of distance between time interval end points.
- (ii) in main program, accumulator for number of points in each linear approximation of tangent.
- (iii) dummy variable in the ENTER instructions when they are used as a signal to the user.

Z: counter for number of signals.

- (i) in subroutine "PEAKS", if $z = 1$ skips print-out of x coordinates of peak positions.
- (ii) in main program, if $z = 3$ go to calculation and print-out of lags between signals 2 and 3.

R0: (i) in subrouting "SETUP", input register for 1st end-point of time interval.

- (ii) in main program, y intercept for 1st tangent line.

R1: (i) in subroutine "SETUP", input register for 2nd end-point of time interval.

- (ii) in main program, slope of 1st tangent line.

R2: y intercept for 2nd tangent line.

R3: slope for 2nd tangent line.

R4: y intercept for 3 tangent line.

R5: slope for 3rd tangent line.
 R6: x coordinate of peak 1 of current signal. Calculated in "PEAKS".
 R7: x coordinate of peak 2 of current signal. Calculated in "PEAKS".
 R8: storage for x coordinate of peak 1 of previous signal.
 R9: storage for x coordinate of peak 2 of previous signal.
 R10: not used.
 R11: not used.
 R12: $\sum x_i$ when accumulating for least-squares.
 R13: $\sum y_i$ when accumulating for least-squares.
 R14: $\sum x_i^2$ when accumulating for least-squares.
 R15: $\sum y_i^2$ when accumulating for least-squares.
 R16: $\sum x_i y_i$ when accumulating for least-squares.
 R17: denominator for least-squares calculation, i.e., $CR14 - R12R12$.